

Provided for non-commercial research and educational use.
Not for reproduction, distribution or commercial use.

PLISKA

STUDIA MATHEMATICA

ПЛИСКА

МАТЕМАТИЧЕСКИ
СТУДИИ

The attached copy is furnished for non-commercial research and education use only.
Authors are permitted to post this version of the article to their personal websites or institutional repositories and to share with other researchers in the form of electronic reprints.
Other uses, including reproduction and distribution, or selling or licensing copies, or posting to third party websites are prohibited.

For further information on
Pliska Studia Mathematica
visit the website of the journal <http://www.math.bas.bg/~pliska/>
or contact: Editorial Office
Pliska Studia Mathematica
Institute of Mathematics and Informatics
Bulgarian Academy of Sciences
Telephone: (+359-2)9792818, FAX:(+359-2)971-36-49
e-mail: pliska@math.bas.bg

NUMERICAL SIMULATION OF THE FLOW AROUND TWO BLUFF BODIES SEPARATED BY A GAP*

Kostadin Filipov, Sonia Tabakova

The aim of the present work is to study numerically the shielding effects of a semi-infinite cylinder and a protruding disk placed in an incompressible viscous flow. The continuity and momentum equations are solved numerically for different flow regimes: laminar and turbulent using the CFD software ANSYS/FLUENT. Different geometrical parameters (diameters and gap aspect ratios) and a wide spectrum of the Reynolds numbers: $5 \leq Re \leq 5 \times 10^5$ are considered. The results for the drag force coefficient and the axial velocity patterns are compared with the classical experimental results of Koenig and Roshko [5] at $Re = 5 \times 10^5$.

1. Introduction

The hydrodynamic or aerodynamic interaction between rigid bodies is a fundamental problem in fluid mechanics. It strongly depends on the following variables connected with the bodies: (a) their shapes and sizes; (b) the distances between them; (c) their orientation with respect to each other; (d) their individual orientation relative to the active external forces; (e) their velocities and spins relative to the undisturbed fluid motion. Usually instead of these dimensional variables, the studies are performed on the basis of non-dimensional parameters, such as: Reynolds number, Re , normalized sizes of the bodies and distances between them with respect to reference body dimension, etc.

2010 *Mathematics Subject Classification*: 76D05, 76M12.

Key words: numerical solution, hydrodynamic interaction, drag coefficient

*The authors acknowledge the possibility to use the software ANSYS/FLUENT bought by the research project I 02/03 of the bulgarian NSF

For example, the hydrodynamic interaction of two rigid spheres in a uniform Stokes flow has been analytically investigated firstly by Davis et al. [1]. For higher Reynolds numbers the same problem is studied only numerically [2]. The obtained numerical results show that the drag force acting on each of the spheres is smaller than the same force experienced on a single sphere and the drag on the front sphere is greater than on the rear one.

The numerical study of the flow around two bluff bodies separated by a gap is of particular interest, because it shows the physical forces acting on the system of bodies and also it can give an idea of how the flow affects them. The symmetry and dimensions of the bodies is of great importance if we are considering the drag coefficient and its eventual reduction. The analysis of a system containing two separated bodies, as opposed to a single body is of high significance, mainly because the front body seems to act as a shield with respect to the rear body reducing the flow separation and drag. Possibly the first experiments of this kind were made in [3], where the effect of the spacing of two disks, arranged coaxially in a stream, on the drag has been studied. The same configuration has been reinvestigated experimentally in [4]. It has been shown that the proper sizing of the disk diameters and of the gap between them leads to significant drag reductions up to 81% lower than that of a disk alone. This experiment shows also the phenomenon of protection of the one body by the other, which has high practical use and further investigation of this matter can give valuable information to developers for fluid flow control.

A similar experiment was done by Koenig and Roshko in [5] concerning the shielding effects of various disks placed coaxially upstream of an axisymmetric flat-faced cylinder. This experiment showed a remarkable decrease of the drag of such a system, for certain combinations of the basic geometric parameters: the diameter and gap ratios.

In parallel with the experimental laboratory analysis of flow around multiple bluff bodies, numerical simulations with three-dimensional CFD (Computational Fluid Dynamics) modeling are performed. However, such models are relatively not well developed by researchers, possibly because the flow around a single bluff body is already difficult enough. Only the experimental and numerical works of Isaev and coworkers [6], [7], [8] concern both the two disks and the disk-cylinder tandem problems.

The aim of the present work is to study numerically the shielding effects of a disk and a semi-infinitely long cylinder axially placed in a flow for different numbers of Reynolds, Re . For the simulation the CFD software ANSYS/FLUENT package is implemented. We use the geometry described in [5] in order to com-

pare our numerical results for the drag force coefficient and the flow visualization patterns with the experimental correspondents of [5] for $Re = 5 \times 10^5$.

2. Problem statement

We shall consider both cases: the flow field around a semi-infinite cylinder and around a tandem body (constructed by a semi-infinite cylinder as a rear body and a disk mounted coaxially as a front body, separated by a gap). The cylinder has a diameter d_2 , the disk is assumed infinitely slim with diameter d_1 and the gap width is g , as shown in Fig.1. The flow to which the cylinder or tandem body are subjected to, is uniform with velocity V . The fluid is assumed viscous incompressible with constant density ρ and constant dynamic viscosity μ . The gravity force and temperature dependence are further neglected.

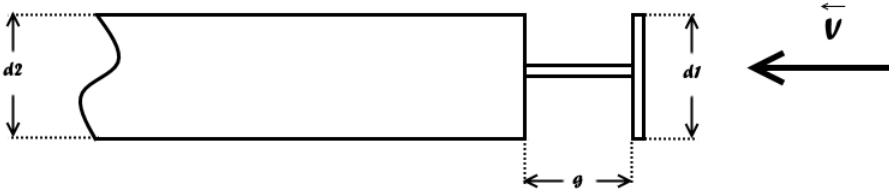


Figure 1: Geometry sketch

The general equations of motions and continuity in dimensionless vector form are the following:

$$(1) \quad \frac{\partial \mathbf{v}}{\partial t} + \mathbf{v} \cdot \nabla \mathbf{v} = -\nabla p + \frac{1}{Re} \nabla \cdot \mathbf{D},$$

$$(2) \quad \nabla \cdot \mathbf{v} = 0,$$

where \mathbf{v} is the velocity vector, p is the pressure, t is the time, $Re = \frac{\rho V d_2}{\mu}$ and $\mathbf{D} = 0.5[\nabla \mathbf{v} + (\nabla \mathbf{v})^T]$ is the strain rate tensor.

The boundary conditions on the tandem body cylinder-disk are the no-slip ones.

3. Numerical results

The described 3D problem with eqs.(1) and (2) and the corresponding boundary conditions is solved numerically using the software ANSYS/FLUENT [9]. Depending on the Reynolds number, the two different models of laminar (for $Re < 1000$) and turbulent $k - \varepsilon$ (for $Re > 1000$) regimes are applied. The cylinder diameter used in the simulations is chosen to be $d_2 = 203mm$. According to [5], the length of the rear body (the cylinder of the tandem body) is taken to be 4 times its diameter, i.e., $L = 812mm$, which is enough to ensure adequate approximation to a semi-infinite body. Therefore the rear end effects on the drag force must be taken off the final result of the drag force coefficient $c_D = 8F_z/\rho V^2\pi d_2^2$, as it is given by the following expression [5]:

$$(3) \quad c_D = \frac{8(F_z - F_{z_{rear}})}{\rho V^2\pi d_2^2},$$

where by F_z the total force acting on the z axis is denoted, while $F_{z_{rear}}$ is the force acting on the rear surface of the cylinder.

Different values of the gap and disk diameter are used for the simulations, which are grouped in 3 main groups and given in Table 1.

Table 1. Considered geometrical cases of the tandem body

case	ratio d_1/d_2	subcase	ratio g/d_2
1	1	1a	1
	1	1b	0.5
	1	1c	0.25
2	0.5	2a	1
	0.5	2b	0.5
	0.5	2c	0.25
3	0.25	3a	1
	0.25	3b	0.5
	0.25	3c	0.25

The calculations are performed in a bounding box around the cylinder or tandem body with sizes 4–5 times greater than its dimensions, such that the velocity on the box walls remains the undisturbed one. The used meshes in the box domain consist of 109098 nodes and 76706 elements for the cylinder case and of 108035 nodes and 19612 elements for the tandem case.

3.1. Velocity Visualization

The numerical results for the axial velocity, v_z , contours are plotted in Figures 2 and 3 for $Re=5 \times 10^5$ and $Re=5 \times 10^2$, respectively. The flow around a single

cylinder is illustrated in Figures 2a and 3a, where the separation region, originating at the shoulder, may be seen. Flow patterns with a disk as a front body of the cylinder are illustrated in Figures 2b, 2d, 3b and 3d for different disk diameters at constant gap width ratios $g/d_2 = 1$, correspondent to cases 1.a and 3.a. It is evident that the separation zone is located in the space between the disk and the cylinder and the flow is attached near at the sharp edge or even at the shoulder of the cylinder without further detachment from the cylinder surface. However, for some combinations of the geometrical parameters, for example for case 2.b, as seen in Figures 2c and 3c, the vortices remain closed in the gap region and almost no separation from the cylinder surface can be seen. With the increase of the diameters' ratio from 0.25 to 1, the vortex region augments significantly. It has been expected the flows to be unsteady, mainly only because of the oscillating turbulent wake after the cylinder. In fact, although that the simulations have been performed with transient model, the solutions converge without visible changes in the velocity contour structure, which means that almost no oscillation has been observed. The reason for this observation can be attributed to the tandem body structure in contrast to the single cylinder. As a whole, the patterns show a qualitative agreement with respect to the flow visualizations obtained experimentally in [5] for $Re=5 \times 10^5$.

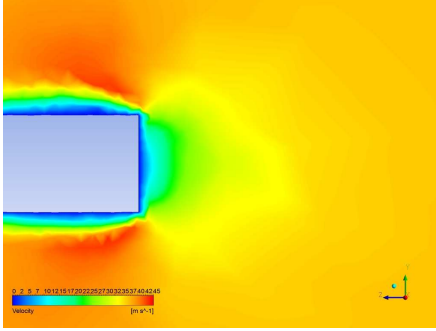
Changing the Reynolds number values, Re (in the performed simulations $5 \times 10^5 \geq Re \geq 5$), the flow changes from steady laminar to unsteady turbulent. At $Re = 5$ for the discussed cases, no separation is present and the flow field resembles to a typical potential streaming. However, with the increase of Re a separation from the disk edges starts and forms a vortex wake, which occupies a small region of the gap, as this is seen for $Re = 5 \times 10^2$ in Figure 3, up to the whole gap region, as shown in Figure 2.

3.2. Drag coefficient

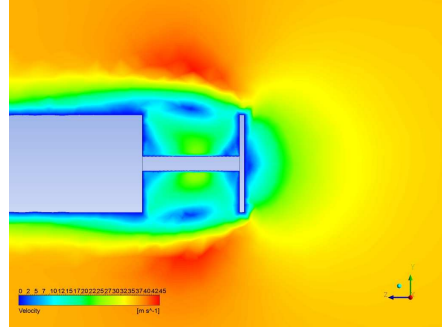
The drag force coefficient c_D has been chosen as a goal of our numerical simulations. First we shall systemize the results obtained from the simulations for different tandem body dimensions and compare them to the existing results from [5]. These results are obtained at $Re=5 \times 10^5$ (a high turbulent flow) using the equation (3). Since we dispose only with the experimental results of [5] for the considered problem, this comparison will play the role of a verification of our numerical solution. In Table 2 the numerical values of the drag coefficient c_D obtained from simulations and experiment at $Re=5 \times 10^5$ are presented for the considered cases. For a fixed diameters' ratio, there exists an optimal gap width, as reported in [5], which is not a linear function of the gap ratio, g/d_2 .

Table 2

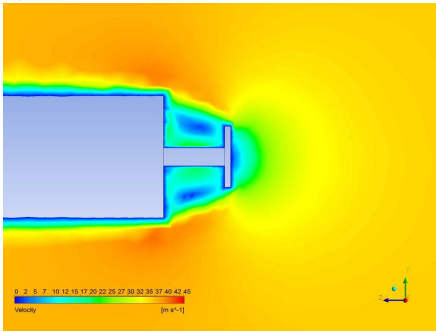
case	subcase	simulation c_D	experimental c_D [5]
1	1a	0.73	0.69 (0.72)
	1b	0.72	0.71 (0.74)
	1c	0.76	0.72 (0.75)
2	2a	0.30	0.24 (0.27)
	2b	0.26	0.25 (0.28)
	2c	0.40	0.39 (0.42)
3	3a	0.36	0.32 (0.35)
	3b	0.49	0.42 (0.45)
	3c	0.66	0.64 (0.67)
cylinder		0.76	0.72 (0.75)



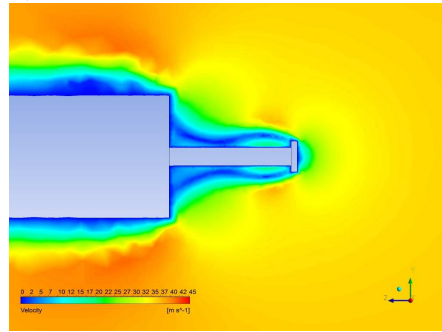
a)



b)



c)



d)

Figure 2: Velocity visualization at $Re=5 \times 10^5$: a) cylinder; b) case 1a; c) case 2b; d) case 3a

According to the numerical results in Table 2, it is evident that with the increase with g/d_2 , the drag coefficient c_D decreases. The drag coefficient values obtained

experimentally in [5] are corrected with the values given in brackets after taking into account the error ± 0.03 due to some measurement restrictions. Note, that the measured $c_D = 0.72$ for a single cylinder becomes 0.75 after the correction. This value is in the range of values $[0.7, 0.8]$ obtained by different experimental methods as reported in [5], [10]. The minimum drag value correspondent to the considered cases occurs for the case 2.b, which is 63% lower than the drag value for a single cylinder. Since the experimental difference between the drags of the case 2.a and 2.b is very small, we accept the case 2.b as that of the numerically calculated drag with the minimum value.

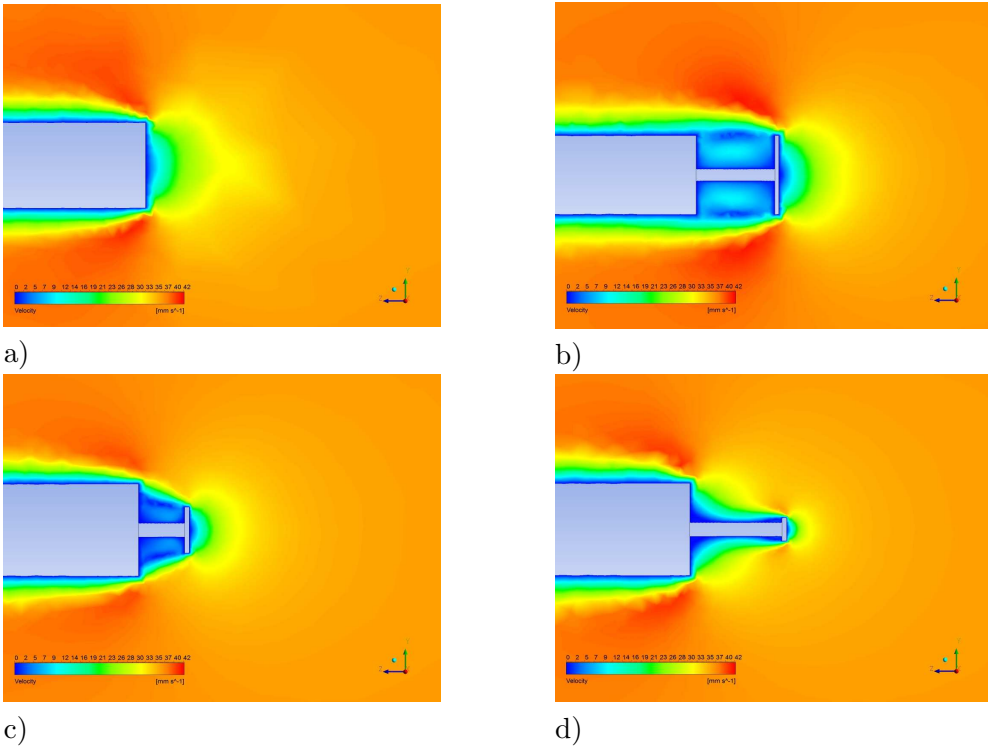


Figure 3: Velocity visualization at $Re=5 \times 10^2$: a) cylinder; b) case 1a; c) case 2b; d) case 3a

The maximum relative difference (error) between the numerical and measured uncorrected drag coefficients is 25% for the case 2.a. If the corrected experimental values are used instead, the maximum error becomes 11.1%. The average maximum relative difference (error) between the numerical and measured uncorrected drag coefficients is around 8.2%, while with corrected drag coefficients, it is

around 4.3%. This means that the simulation is in good correspondence with the existing experiments. Here, we would like to mention the difficulties connected with the simulation performance, which are mainly due to the mesh generation and subsequent refinements. The presented results have been obtained as optimal after applying different meshes.

Table 3

case	subcase	$Re=50$	$Re=5 \times 10^2$	$Re=5 \times 10^3$	$Re=5 \times 10^4$	$Re=5 \times 10^5$
1	1a	3.67	1.45	0.81	0.74	0.73
	1b	3.45	1.28	0.75	0.72	0.72
	1c	3.36	1.25	0.78	0.76	0.76
2	2a	3.39	1.14	0.40	0.33	0.30
	2b	3.20	1.01	0.35	0.28	0.26
	2c	3.23	1.05	0.48	0.43	0.40
3	3a	3.28	1.12	0.50	0.38	0.36
	3b	3.21	1.12	0.54	0.49	0.49
	3c	3.21	1.15	0.69	0.66	0.66
cylinder		2.93	0.88	0.77	0.76	0.76

The experimental results concern only very high Reynolds numbers of order 10^5 and do not give any insight how the drag coefficient changes with Re . For a more clear representation of how the drag coefficient c_D is affected by the change in the Reynolds number, simulations have been made for different Re . The cylinder and tandem body c_D change can be seen in Table 3 and Fig.4. The simulation results clearly show the dependency as expected. With the decrease of the Reynolds number (i.e. of the flow velocity), the drag coefficient c_D increases in value. We can also denote that for highly turbulent flows ($Re > 5 \times 10^3$) c_D tends to remain almost constant for all discussed cases. The drag coefficient as a function of Re has a reasonable behavior with respect to the drag coefficients of other axisymmetric bodies [11].

4. Conclusions

The shielding effect of a disk and a semi-infinite cylinder (a tandem body) axially placed in a viscous incompressible flow is studied numerically by use of the software ANSYS/FLUENT through different geometric parameters and a wide spectrum of Reynolds numbers: $5 \leq Re \leq 5 \times 10^5$.

The axial velocity visualization is qualitatively similar to the experimentally visualized flow at $Re = 5 \times 10^5$ in [5]. The drag coefficient for both the cylinder and tandem body is calculated due to the numerical results. The comparison of its values with the experimentally obtained values at $Re = 5 \times 10^5$ in [5] is

good. New results for the drag coefficient dependence on the Reynolds number for an axially placed infinite cylinder with and without a disk as a front body in a viscous incompressible flow are also obtained.

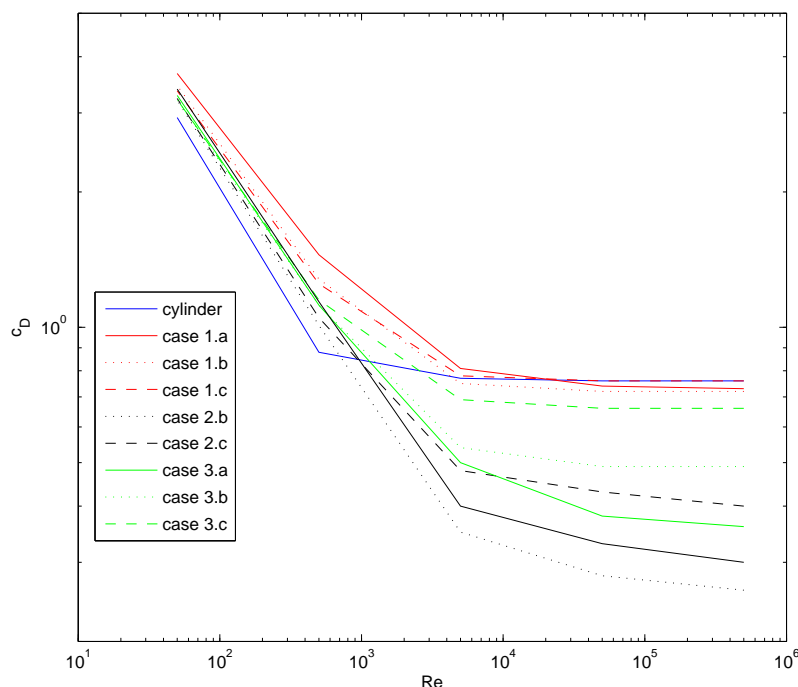


Figure 4: Drag force coefficients c_D at different Reynolds numbers

References

- [1] A. M. J. DAVIS, M. E. O'NEIL, J. M. DORREPAAL, K. RANGER. Separation from the surface of two equal spheres in Stokes flow. *J. Fluid Mech.* **77** (1976), 625–644.
- [2] Z. ZAPRYANOV, S. TABAKOVA. Dynamics of Bubbles, Drops and Rigid Particles. Dordrecht, Boston, London: Kluwer Academic Publishers, 1999.
- [3] G. EIFFEL. Resistance of the Air and Aviation, 2nd edn, pp. 54–60, London, Constable and Co, 1913.

- [4] T. MOREL, M. BOHN. Flow over two circular disks in tandem. *J. Fluids Eng* **102** (1980), 104–111.
- [5] K. KOENING, A. ROSHKO. An experimental study of geometrical effects on the drag and flow field of two bluff bodies separated by a gap. *J. Fluid Mech.* **156** (1985), 167–204.
- [6] S. A. ISAEV. Analysis of the drag of two discs in a turbulent incompressible fluid flow. *Journal of Engineering Physics and Thermophysics* **48**, 2 (1985), 180–184.
- [7] V. K. BOBYSHEV, S. A. ISAEV, O. L. LEMKO. Effect of viscosity on the vortex structure of a flow around a cylinder and the drag of the cylinder with and without a disk in front of it. *Journal of Engineering Physics and Thermophysics* **51**, 2 (1986), 914–920.
- [8] V. K. BOBYSHEV, S. V. GUVERNYUK, S. A. ISAEV. Identification of the vortex mechanism of front stabilization in modeling of asymmetric flow of an incompressible fluid along a cylinder with a protruding disk. *Journal of Engineering Physics and Thermophysics* **72**, 4 (1999), 606–611.
- [9] ANSYS FLUENT Theory Guide, Release 14.0, 2014.
- [10] K. KOENING. Interference effects on drag of bluff bodies in tandem. PhD thesis, California Institute of Technology, Pasadena, California, 1978.
- [11] B. MASSEY, J. WARD-SMITH. *Mechanics of fluids*, Eighth edition. London and New York, Taylor & Fransis, 2006.

Department of Mechanics
Technical University – Sofia
Branch Plovdiv
Plovdiv, Bulgaria

Department of Fluid Mechanics
Institute of Mechanics
BAS, Sofia, Bulgaria
e-mail: stabakova@gmail.com